ISSN 1063-7761, Journal of Experimental and Theoretical Physics, 2011, Vol. 113, No. 1, pp. 113–120. © Pleiades Publishing, Inc., 2011.
Original Russian Text © A.M. Kuz'menko, A.A. Mukhin, V.Yu. Ivanov, A.M. Kadomtseva, S.P. Lebedev, L.N. Bezmaternykh, 2011, published in Zhurnal Eksperimental'noi i Teoreticheskoi Fiziki, 2011, Vol. 140, No. 1, pp. 131–139.

ORDER, DISORDER, AND PHASE TRANSITION IN CONDENSED SYSTEM

Antiferromagnetic Resonance and Dielectric Properties of Rare-earth Ferroborates in the Submillimeter Frequency Range

A. M. Kuz'menko[a], A. A. Mukhin[a,*], V. Yu. Ivanov[a], A. M. Kadomtseva[b], S. P. Lebedev[a], and L. N. Bezmaternykh[c]

[a] *Institute of General Physics, Russian Academy of Sciences, ul. Vavilova 38, Moscow, 119991 Russia*
**e-mail: mukhin@ran.gpi.ru*
[b] *Moscow State University, Moscow, 119991 Russia*
[c] *Kirensky Institute of Physics, Siberian Branch, Russian Academy of Sciences, Akademgorodok, Krasnoyarsk, 660036 Russia*

Received December 10, 2010

Abstract—The magnetoresonance and dielectric properties of a number of crystals of a new family of multiferroics, namely, rare-earth ferroborates $RFe_3(BO_3)_4$ (R = Y, Eu, Pr, Tb, $Tb_{0.25}Er_{0.75}$), are studied in the submillimeter frequency range ($\nu = 3$–$20\ cm^{-1}$). Ferroborates with R = Y, Tb, and Eu exhibit permittivity jumps at temperatures of 375, 198, and 58 K, respectively, which are caused by the $R32 \longrightarrow P3_121$ phase transition. Antiferromagnetic resonance (AFMR) modes in the subsystem of Fe^{3+} ions are detected in the range of antiferromagnetic ordering ($T < T_N = 30$–40 K) in all ferroborates that have either an easy-plane (Y, Eu) or easy-axis (Pr, Tb, $Tb_{0.25}Er_{0.75}$) magnetic structure. The AFMR frequencies are found to depend strongly on the magnetic anisotropy of a rare-earth ion and its exchange interaction with the Fe subsystem, which determine the type of magnetic structure and the sign and magnitude of an effective anisotropy constant. The basic parameters of the magnetic interactions in these ferroborates are found, and the magnetoelectric contribution to AFMR is analyzed.

DOI: 10.1134/S106377611105013X

INTRODUCTION

Rare-earth ferroborates $RFe_3(BO_3)_4$ (R = Y, La–Lu) have recently attracted considerable interest due to the discovery of multiferroelectric phenomena in them [1, 2] and to their interesting magnetic, optical, and other properties caused by the exchange interaction between the iron and rare-earth magnetic subsystems [3, 4]. At sufficiently high temperatures, all rare-earth ferroborates have a noncentrosymmetric trigonal structure belonging to space group $R32$ [5, 6], which remains unchanged in a number of ferroborates with a large ionic radius of an R ion (La–Sm) down to low temperatures. In ferroborates with a smaller ionic radius of an R ion (Eu–Er, Y), a phase transition into a low-symmetry trigonal crystal structure of space group $P3_121$ takes place when temperature decreases [7, 8].

At temperatures below $T_N = 30$–40 K, antiferromagnetic ordering occurs in the iron ion subsystem in ferroborates: depending on the type of R ion, iron ion spins are oriented in either plane *ab* (R = Nd, Sm, Eu, Er, Y) [4, 9, 10] or along trigonal axis *c* (R = Pr, Tb, Dy) [11–14]. In this case, a magnetic order is also induced in the rare-earth subsystem due R–Fe to exchange; it plays an important role in stabilizing an easy-plane or uniaxial magnetic structure, and the role of a rather weak R–R interaction here is insignificant. A strong effect of the anisotropy of the rare-earth subsystem on a magnetic structure and spontaneous and magnetic field–induced phase transitions is indicated by recent studies of substitutional ferroborates $Tb_{1-x}Er_xFe_3(BO_3)_4$ [15] and $Nd_{1-x}Dy_xFe_3(BO_3)_4$ [16] with competing R–Fe exchange interactions.

Obviously, these specific features of the interacting Fe and R subsystems should manifest themselves in not only static magnetic and magnetoelectric properties but also in high-frequency magnetoresonance phenomena, which are scantly known in ferroborates. In particular, a recent magnetoresonance investigation of $Y_{1-x}Gd_xFe_3(BO_3)_4$ ferroborates performed in the millimeter frequency range [17] revealed antiferromagnetic resonance (AFMR) modes of iron ion spins and a significant effect of the Gd subsystem on their frequency and the energy of magnetic anisotropy.

In this work, we present the results of studying the antiferromagnetic resonance and the dielectric properties of ferroborates $RFe_3(BO_3)_4$ (R = Y, Eu, Pr, Tb, $Tb_{0.25}Er_{0.75}$) in the submillimeter frequency range (3–20 cm^{-1}). The main purpose of this work is to reveal the dependence of the AFMR frequency on the magnetic anisotropy of rare-earth ions, to determine their contribution to the effective crystal anisotropy energy, and to investigate the behavior of permittivity (in particular, during a structural phase transition).

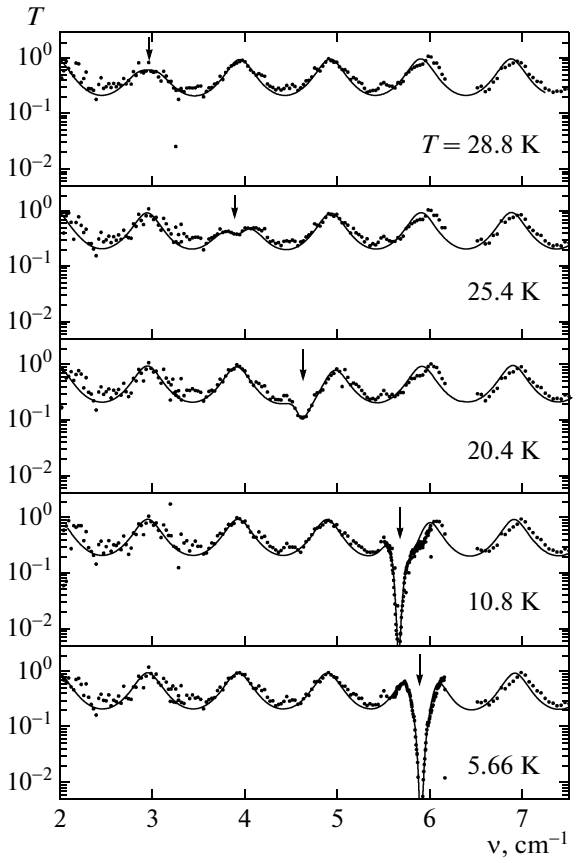

Fig. 1. Evolution of the absorption spectra and the high-frequency AFMR mode (indicated by arrows) in easy-plane $EuFe_3(BO_3)_4$ in the polarization $h \parallel b$ and $e \parallel c$: (points) experiment and (curves) fit.

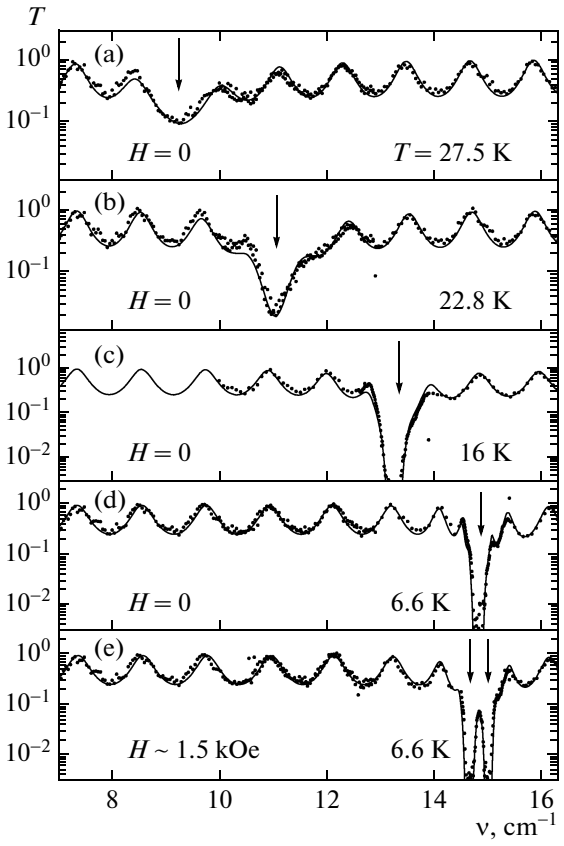

Fig. 2. (a–d) Transmission spectra of easy-axis $TbFe_3(BO_3)_4$ in the polarization $h \parallel b$ and $e \parallel c$ illustrating the temperature behavior of the AFMR mode at $H = 0$. (e) Splitting of the resonance line in a moderate magnetic field $H \parallel c$: (points) experiment and (curves) fit.

EXPERIMENTAL

Ferroborate single crystals up to 1 cm in size were grown upon solidification from a melt on seeds [18]. The samples for quasi-optical studies were prepared in the form of *a*-cut (R = Y, Eu, Tb, $Tb_{0.25}Er_{0.75}$) and *c*-cut (R = Pr) plane-parallel plates 0.5–1 mm thick. The polarization measurements of transmission spectra $T(\nu)$ were carried out using quasi-optical BWT spectroscopy (BWT stands for backward-wave tube) [19] in the frequency range 3–20 cm^{-1} and the temperature range 3–300 K.

Figures 1 and 2 give examples for the temperature evolution of $T(\nu)$ spectra for easy-plane ferroborate $EuFe_3(BO_3)_4$ and easy-axis ferroborate $TbFe_3(BO_3)_4$. All spectra were characterized by oscillations induced by the interference of radiation in a plane-parallel sample. In the antiferromagnetic ordering range ($T < T_N$ = 35–40 K), resonance absorption lines were detected against the background of these oscillations: they were only detected for the polarization of a magnetic field normal to the *c* axis and were identified as AFMR modes of the Fe subsystem (see below). The recorded spectra were simulated with the Fresnel formula for a plane-parallel layer with allowance for the dispersion of magnetic permeability near a resonance absorption line:

$$\mu(\nu) = 1 + \sum_k \Delta\mu_k \nu_k^2/(\nu_k^2 - \nu^2 + i\nu\Delta\nu_k),$$

where ν_k, $\Delta\nu_k$, and $\Delta\mu_k$ are the frequency, line width, and contribution of the AFMR mode to the magnetic permeability. When processing $T(\nu)$ spectra, we obtained the temperature dependences of complex permittivity ε (Fig. 3) and the AFMR mode parameters (Figs. 4, 5).

RESULTS AND DISCUSSION

We first consider the dielectric properties. As is seen in Fig. 3, the temperature dependences of the real part of permittivity ε' of ferroborates $YFe_3(BO_3)_4$, $TbFe_3(BO_3)_4$, and $EuFe_3(BO_3)_4$ exhibit a strong anisotropy along and across trigonal axis *c*. Jumplike anomalies of ε'_c and $\varepsilon'_{\perp c} \equiv \varepsilon'_b$ correspond to the transition from the high-temperature *R*32 phase into the

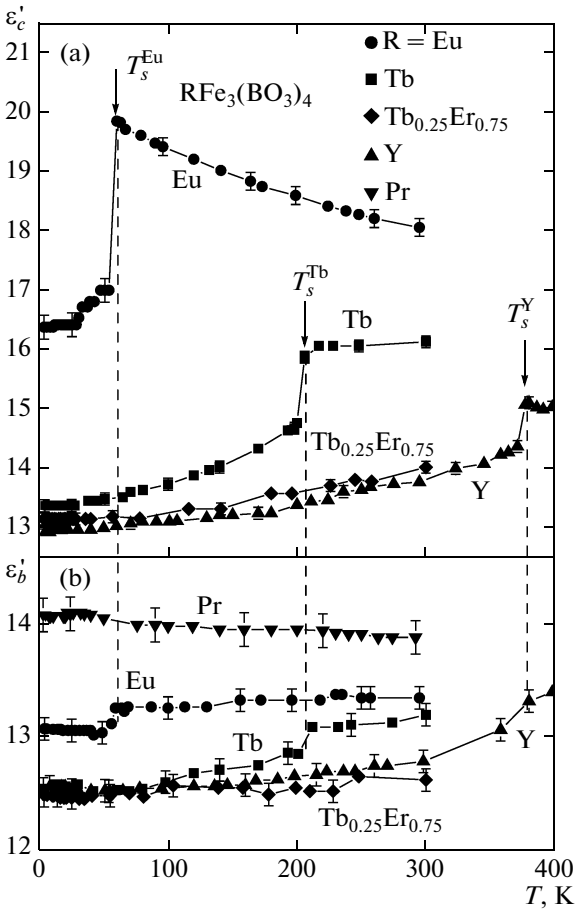

Fig. 3. Temperature dependences of the real part of the permittivity at a frequency of 13 cm^{-1} (390 GHz) (a) along the *c* axis and (b) in the perpendicular direction for ferroborates with R = Y, Eu, Pr, Tb, and $Tb_{0.25}Er_{0.75}$. Arrows indicate the phase-transition temperatures.

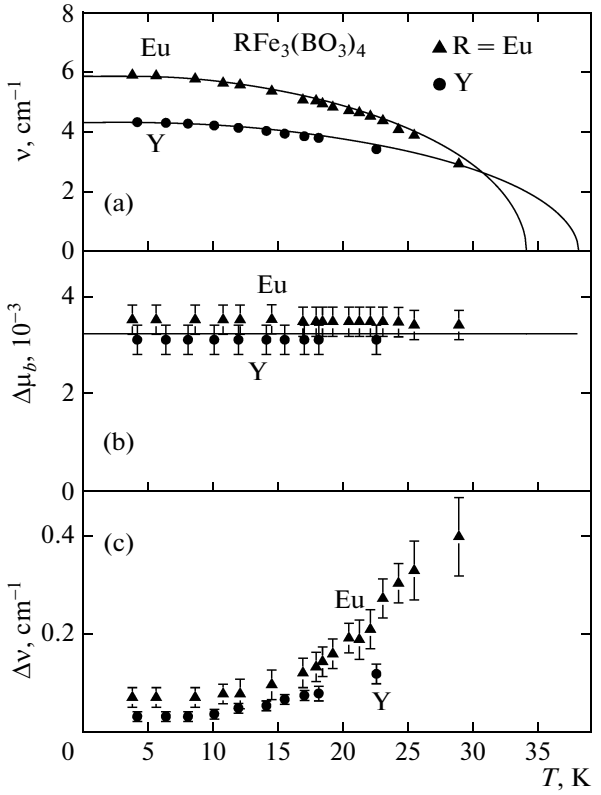

Fig. 4. Temperature dependences of resonance frequencies ν, mode contributions to magnetic permeability $\Delta\mu_b$, and linewidth Δν of the high-frequency AFMR modes ($h \parallel b$) in easy-plane $YFe_3(BO_3)_4$ and $EuFe_3(BO_3)_4$ ferroborates: (points) values obtained from transmission spectra and (lines) calculation.

$P3_121$ phase with lower symmetry. Phase-transition temperatures T_s are 375 K in $YFe_3(BO_3)_4$, 198 K in $TbFe_3(BO_3)_4$, and 58 K in $EuFe_3(BO_3)_4$, which agrees well with the data obtained from heat capacity in [6, 13]. The most pronounced permittivity jumps are observed along the trigonal axis. When the temperature decreases, the $\varepsilon_c'(T)$ dependence changes its character below phase-transition temperature T_s and becomes descending, whereas it increases or remains almost unchanged above T_s. In the composition $Tb_{0.25}Er_{0.75}Fe_3(BO_3)_4$, the behavior of $\varepsilon_{\perp c}'$ corresponds to the low-temperature $P3_121$ phase at $T \le 300$ K, which is likely to indicate a structural phase transition above room temperature. Quantity $\varepsilon_{\perp c}'$ changes weakly with temperature, exhibits a small jump during the structural transition, and falls in the range $12 < \varepsilon_{\perp c}' < 14$ for all compositions under study. As for the frequency dependence of the permittivity in the frequency range 2–16 cm^{-1}, it is very weak or absent. The imaginary part of the permittivity (Fig. 3b) is less than 0.1–0.2 at room temperature for all ferroborates under study, decreases significantly with decreasing temperature, and exhibits small anomalies during structural phase transitions. A similar character of the temperature dependences of permittivity was also observed at low (radio) frequencies [4, 7].

Let us now consider the magnetoresonance properties. The easy-plane antiferromagnetic state has the following two AFMR modes [20]. In the low-frequency mode, the oscillations of antiferromagnetism vector **L** lie in easy plane *ab* and are excited by a field parallel to axis *c*,

$$\left(\frac{\omega_1}{\gamma}\right)^2 \approx H^2 + 2H_E H_{A6}^{\mathrm{Fe}} \cos 6\varphi. \qquad (1)$$

The high-frequency mode corresponds to antiferromagnetic moment **L** oscillations deviated from the basal (easy) plane and excited by a field normal to axis *c* and vector **L**,

$$\left(\frac{\omega_2}{\gamma}\right)^2 \approx 2H_E H_A^{\mathrm{Fe}} \equiv \frac{K_{\mathrm{Fe}}}{\chi_\perp}. \qquad (2)$$

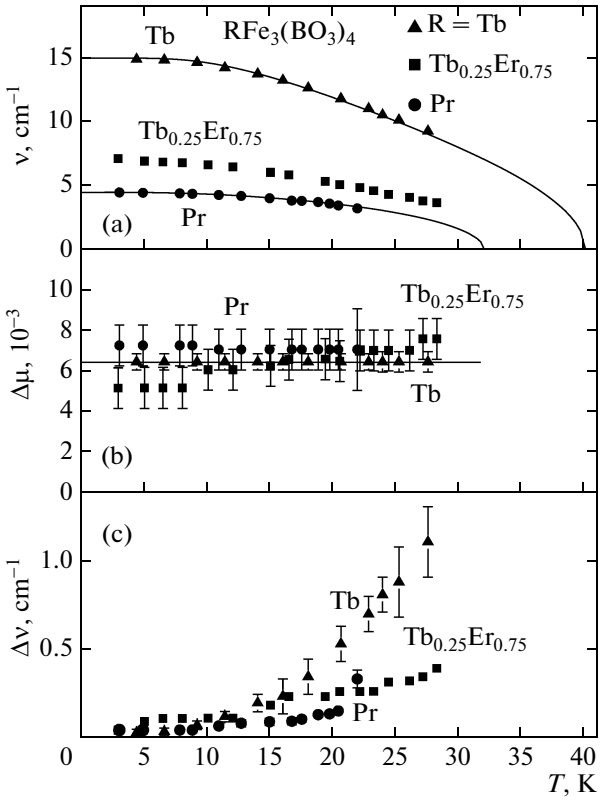

Fig. 5. Temperature dependences of resonance frequencies ν, mode contributions to magnetic permeability $\Delta\mu_b$, and linewidth Δν of the AFMR mode in uniaxial $PrFe_3(BO_3)_4$, $TbFe_3(BO_3)_4$, and $Tb_{0.25}Er_{0.75}Fe_3(BO_3)_4$ ferroborates: (points) values obtained from transmission spectra and (lines) calculation.

In Eq. (1), an applied magnetic field lies in the basal plane and, at $H \gg H_{A6}^{Fe}$, determines the orientation of **L** in this plane, which is specified by angle φ (**H** ⊥ **L**); $\chi_\perp$ is the transverse susceptibility of antiferromagnetically ordered iron spins; M_0 is the magnetization of the iron spin sublattices; $H_E = M_0/2\chi_\perp$ is the field of isotropic Fe–Fe exchange; $H_A^{Fe} = K_{Fe}/M_0$ is the anisotropy field of the iron subsystem, which stabilizes the easy-plane state; H_{A6}^{Fe} is the anisotropy field in the basal plane ($H_{A6}^{Fe} \ll H_A^{Fe} \ll H_E$); and γ is the gyromagnetic ratio.

In the easy-plane ferroborates $YFe_3(BO_3)_4$ and $EuFe_3(BO_3)_4$, the modes excited by a field parallel to axis *b* are identified as high-frequency AFMR modes of Fe^{3+} ions (Fig. 1). In $YFe_3(BO_3)_4$ with nonmagnetic Y, the obtained values of frequency $\nu_2 = \omega_2/2\pi$ and contribution Δμ (Figs. 4a, 4b) are only determined by the iron subsystem. The contribution of the high-frequency mode excited by ac magnetic field **h** along any direction **n** in the basal lane is determined by the expression ($H = 0$)

$$\Delta\mu_n = 4\pi\chi_\perp[1 - \langle(\mathbf{L}\cdot\mathbf{n})^2\rangle] = 4\pi\chi_\perp/2, \qquad (3)$$

where averaging is performed over all vector **L** directions with allowance for a uniform distribution in the *ab* plane over six natural anisotropy directions. (This expression also holds true for a continuous distribution of **L** in this plane caused by random elastic stresses if their magnetoelastic contribution to the energy induced in the basal plane exceeds natural anisotropy H_{A6}^{Fe}.) Such a distribution is supported by the anisotropy of static magnetic susceptibility of $YFe_3(BO_3)_4$, where the susceptibility in the basal plane is half that along the *c* axis [4]. Note also that the obtained contribution (Fig. 4b) is almost temperature independent, which agrees with Eq. (3). With this contribution of mode ν_2, we can determine the static susceptibility ($\chi_\perp \approx (1.2–1.3) \times 10^{-4}$ cm^3/g) and the corresponding exchange field ($H_E = M_0/2\chi_\perp = 680$ kOe), which agree well with the results of static measurements [4]. Using the value of mode ν_2, we can calculate the anisotropy constant of the iron subsystem ($K_{Fe} = 2.7 \times 10^5$ erg/g), which agrees with the data in [17]. The temperature dependence $\nu_2(T)$ (Fig. 4a) can be described using the molecular field approximation for the magnetizations of the iron sublattices.

The second (low-frequency) AFMR mode, which is controlled by the anisotropy in easy plane *ab*, has a much lower frequency and does not manifest itself in the frequency range under study. The mode frequency increases in a magnetic field $H \perp c$; therefore, this mode was detected in [17] at a fixed frequency by sweeping magnetic field.

Generally speaking, when analyzing ferroborates with rare-earth ions, one should consider two interrelated magnetic subsystems, whose dynamics depends substantially on the relation between the natural resonance frequencies of the subsystems. In the case of the ferroborates under study (where the characteristic electron transition frequencies in the rare-earth system (ω_R) are significantly higher than the AFMR frequencies of the Fe subsystem (ω_{Fe})), we can assume that the dynamic variables of the R subsystem at frequencies on the order of ω_{Fe} immediately follow iron ion spins and are determined by the corresponding effective fields. As a result, we can exclude the R subsystem at frequencies on the order of ω_{Fe} variables and describe their contribution using an effective thermodynamic potential depending only on the Fe subsystem variables, which was used to analyze the dynamic properties of other similar systems (e.g., orthoferrites) [19, 21]. If the exchange splitting (shift)

of the R ion levels caused by the R–Fe interaction is significantly smaller than the characteristic distances between R ion levels $\hbar\omega_R$ in a crystal field, we can write the free energy as

$$\Phi \approx \Phi_{\rm Fe} - \frac{1}{4}\sum_{\alpha=\pm} \mathbf{H}^{\alpha}_{\rm eff}\hat{\chi}^{R}\mathbf{H}^{\alpha}_{\rm eff}, \quad (4)$$

where $\hat{\chi}^{R}$ is the tensor of the static magnetic susceptibility of the rare-earth ion in the crystal field, $\mathbf{H}^{\pm}_{\rm eff} = \mathbf{H} + \mathbf{H}^{\pm}_{\rm ex}$, and $\mathbf{H}^{\pm}_{\rm ex} \approx \pm(\lambda_\perp L_x, \lambda_\perp L_y, \lambda_\parallel L_z)$ is the R–Fe exchange field in which the contribution proportional to ferromagnetic moment M of the Fe subsystem is omitted because of $M \ll L$, and signs "±" correspond to two R sublattices. In this case, the anisotropy energy can be described by effective anisotropy constant $K_{\rm eff}$, which includes both the anisotropy of the iron spin subsystem and the contribution of the rare-earth subsystem,

$$\Phi_A = \frac{1}{2}K_{\rm Fe}L_z^2 - \frac{1}{2}(\chi_\parallel^R\lambda_\parallel^2 - \chi_\perp^R\lambda_\perp^2)L_z^2 \equiv \frac{1}{2}K_{\rm eff}L_z^2. \quad (5)$$

This approach can be used to analyze the AFMR in $EuFe_3(BO_3)_4$, since the ground state of the Eu^{3+} ion is nonmagnetic ($J = 0$) and separated from excited multiplets by a significant energy interval ($\Delta^{\rm Eu} \approx 400$ cm^{-1} [22]) and its magnetic properties are determined by an admixture of excited states (Van Vleck magnetism) [23]. The increase in frequency ν_2 in $YFe_3(BO_3)_4$ as compared to $YFe_3(BO_3)_4$ (Fig. 4a) indicates an additional contribution of Eu^{3+} ions to the anisotropy energy. We assume that this contribution is mainly related to the anisotropy of the Van Vleck magnetic susceptibility of the Eu^{3+} ion [4], for which $\chi_{\perp c}^{VV} > \chi_c^{VV}$ [4], and easily explain the increase in the effective anisotropy constant $K_{\rm eff} = K_{\rm Fe} + (\chi_{\perp c}^{VV} - \chi_c^{VV})H_{\rm Eu-Fe}^2$ (where $H_{\rm Eu-Fe}$ is the field of the isotropic Eu–Fe exchange) by a positive contribution of the europium subsystem. We now use the frequency and the contribution of mode ν_2 obtained above, the anisotropy of the magnetic susceptibility of $EuFe_3(BO_3)_4$ [4], and the value of $K_{\rm eff}$ obtained above and find $H_{\rm Eu-Fe} \approx 140$ kOe. The temperature dependence of frequency ν_2 is qualitatively similar to that of yttrium ferroborate and is also described in the molecular field approximation (Fig. 4a).

In the easy-axis state ($\mathbf{L} \parallel \mathbf{c}$), which takes place in ferroborates $PrFe_3(BO_3)_4$ [12], $TbFe_3(BO_3)_4$ [10, 13, 24], and $Tb_{0.25}Er_{0.75}Fe_3(BO_3)_4$ [15], two AFMR modes are excited in the polarization $h \perp c$ [20], and their frequencies (at $H \parallel c$) are

$$\omega^{\pm} \approx \gamma(\sqrt{2H_E H_A^{\rm eff}} \pm H), \quad (6)$$

where $H_A^{\rm eff} = -K_{\rm eff}/M_0$ is the effective anisotropy field, which stabilizes the easy-axis state at $K_{\rm eff} < 0$. In the absence of a field, resonance frequencies are degenerate, $\omega_0 = \omega^+ = \omega^-$, and one absorption line is detected in polarization $h \perp c$ (Fig. 2); its contribution is determined by the transverse susceptibility of iron spins $\Delta\mu_{\perp c} = 4\pi\chi_\perp$.

According to the optical data in [11], the ground state of the Pr^{3+} ion in $PrFe_3(BO_3)_4$ in the crystal field is singlet and the energy of the next excited state corresponds to 48 cm^{-1}, which allows us to analyze the AFMR in the iron subsystem using effective thermodynamic potential (4) and anisotropy energy (5). The contribution of the detected mode to the magnetic permeability (Fig. 5b) gives the values of $\chi_\perp$ and H_E that are close to the corresponding parameters of $YFe_3(BO_3)_4$. With the frequency of the detected mode (Fig. 5a) and the obtained value of H_E, we can find the constant ($K_{\rm eff} = -2.7 \times 10^5$ erg/g) and the corresponding spin-flop transition field ($H_{\rm sf} = [-K_{\rm eff}/\chi_\perp]^{1/2} \approx 48$ kOe), which agree well with the data obtained from low-temperature magnetization curves [12]. According to magnetic measurements, the susceptibility of Pr ions is strongly anisotropic and $\chi_c^{\rm Pr} > \chi_{\perp c}^{\rm Pr}$, which is likely to be the main cause of the change in the sign of the effective anisotropy constant and the stabilization of the uniaxial state. Nevertheless, we should not rule out the contribution of the anisotropic part of the Pr–Fe exchange revealed from the optical data in [11].

We found in $TbFe_3(BO_3)_4$ a significant increase in the AFMR mode frequency (Fig. 5a), which indicates not only a change in the sign of effective anisotropy constant $K_{\rm eff}$ but also its high value due to the anisotropic contribution of Tb^{3+} ions, which are polarized along their Ising axis (coinciding with the trigonal axis of the crystal). An easy-axis character of the magnetic ordering in $TbFe_3(BO_3)_4$ is supported by the fact that the AFMR mode detected in the polarization $h \perp c$ is split into two modes in applied magnetic field H (Fig. 2e), according to Eq. (6). The ground state of the Tb^{3+} ion in the crystal field is a quasi-doublet, whose splitting is almost completely determined by the exchange field [13, 15],

$$2\Delta_{\rm Tb} = 2\mu_{\rm Tb}^z H_{\rm Tb-Fe}^z = 2\mu_{\rm Tb}^z(\lambda_\parallel L_z),$$

and the contribution to the free energy is

$$\Phi_{\rm Tb} \approx -NTk_{\rm B}\ln 2\cosh(\Delta_{\rm Tb}/k_{\rm B}T),$$

where N is the number of Tb ions. Taking into account a high value of this exchange splitting ($2\Delta_{\rm Tb} \approx 30$ cm^{-1} [13, 15]) as compared to the detected AFMR frequencies (Fig. 5a), we can calculate them using the Landau–Lifshitz equations by allowing for rare-earth contribution $\Phi_{\rm Tb}$ to the total thermodynamic potential of the system. For the resonance frequencies, this gives an expression whose form coincides with Eq. (6) and

the effective anisotropy constant in which contains a negative contribution of Tb,

$$K_{\text{eff}} \equiv K_{\text{Fe}} - N\Delta_{\text{Tb}}\tanh(\Delta_{\text{Tb}}/k_{\text{B}}T) < 0.$$

The values of field H_E and $\chi_\perp$ for $TbFe_3(BO_3)_4$ that are determined by the contribution of the AFMR mode to magnetic permeability $\Delta\mu_{\perp c}$ (Fig. 5b) turn out to be close to the corresponding values in the other ferroborates. Using these data and the values of AFMR frequency ω_0 at a low temperature and K_{Fe} found for yttrium ferroborate, we can determine the exchange splitting,

$$2\Delta_{\text{Tb}} = [\chi_\perp(\omega_0/\gamma)^2 - K_{\text{Fe}}]/N \approx 30\ \text{cm}^{-1}$$

and the corresponding exchange field ($H^c_{\text{Tb–Fe}} \approx 35$ kOe), which agree well with the results of static investigations [13, 15] (in particular, with the spin-flop transition field [15, 24]. Note that it is impossible to directly observe resonance transitions in the ground quasi-doublet because of the Ising character of the Tb^{3+} ion.

This picture of the formation of magnetic anisotropy in $TbFe_3(BO_3)_4$ is supported by the behavior of AFMR in the dilute $Tb_{0.25}Er_{0.75}Fe_3(BO_3)_4$ system. The twofold decrease in the AFMR frequency detected in it (Fig. 5a) supports the prevailing contribution of Tb^{3+} ions to the effective anisotropy even for their fourfold dilution. The contribution of Er^{3+} here is not very significant because of a smaller exchange splitting (about 1.9 cm^{-1} [10]).

This analysis of the magnetoresonance properties of the ferroborates was performed without allowance for a magnetoelectric interaction, since we failed to detect the manifestation of the corresponding magnetoelectric phenomena in the frequency range under study. Nevertheless, we will briefly discuss these interesting fine effects and analyze their observation conditions.

The magnetoelectric contribution of the Fe subsystem to the thermodynamic potential has the form [1, 2]

$$\begin{aligned}\Phi_{ME} &= -c_1(P_xL_yL_z - P_yL_xL_z)\\ &- c_2[P_x(L_x^2 - L_y^2) - 2P_yL_xL_y]\\ &- c_6P_zL_xL_z(L_x^2 - 3L_y^2),\end{aligned} \quad (7)$$

where $\mathbf{P}$ is the electric polarization and $c_{1,2,6}$ are constants. We add Φ_{ME} and dielectric part $\Phi_E = -\mathbf{P}\cdot\mathbf{E} + (1/2)\mathbf{E}\hat{\chi}^E\mathbf{E}$ to the total thermodynamic potential and use the equations of motion for dynamic variables $\mathbf{M}$, $\mathbf{L}$, and $\mathbf{P}$ in order to determine the total linear response of the system to an ac magnetic and electric field,

$$\mathbf{m} = \hat{\chi}^m\mathbf{h} + \hat{\chi}^{me}\mathbf{e}, \quad \mathbf{p} = (\tilde{\hat{\chi}}^{me})^*\mathbf{h} + \hat{\chi}^e\mathbf{e},$$

where $\hat{\chi}^m$, $\hat{\chi}^e$, and $\hat{\chi}^{me}$ are the magnetic, electric, and magnetoelectric susceptibilities of the system, respectively. In the uniaxial state, these susceptibilities are diagonal and have a resonance contribution,

$$\begin{aligned}\chi^m_{xx,yy} &\equiv \chi^m_\perp = \chi_\perp R(\omega),\\ \chi^e_{xx,yy} &\equiv \chi^e_\perp = \chi^E_\perp + \Delta\chi^e_{\text{rot}}R(\omega),\\ \chi^{me}_{xx,yy} &= i\chi^{me}_\perp \equiv \frac{i\omega}{\omega_0}\sqrt{\chi_\perp\Delta\chi^e_{\text{rot}}}R(\omega),\end{aligned}$$

where $\Delta\chi^e_{\text{rot}} = P_1^2/|K_{\text{eff}}|$ is the magnetoelectric contribution of rotation to the electric susceptibility, $P_1 = c_1\chi^E_\perp L^2_{zo}$, $\chi^E_\perp = (\varepsilon_\perp - 1)/4\pi$ is the lattice part of the electric susceptibility, $R(\omega) = \omega_0^2/(\omega_0^2 - \omega^2 + i\omega\Delta\omega)$, and ω_0 and $\Delta\omega$ are the AFMR mode frequency and width, respectively. The most interesting consequence caused by the magnetoelectric susceptibility is the appearance of two inherent right and left circularly polarized electromagnetic modes characterized by refractive index $n_\pm = n_0 \pm 4\pi\chi^{me}_\perp$, where $n_0 = \sqrt{\varepsilon_\perp\mu_\perp}$, $\varepsilon_\perp = 1 + 4\pi\chi^e_\perp$, and $\mu_\perp = 1 + 4\pi\chi^m_\perp$, during their propagation along the c axis. This leads to the rotation of the polarization plane of a wave through an angle $\Delta\theta_{me} = (\omega d/c)4\pi\chi^{me}_\perp$, where c is the velocity of light, when it passes through a layer of thickness d. We now use the data of magnetoelectric studies of $PrFe_3(BO_3)_4$ [12] and $TbFe_3(BO_3)_4$ [15], which estimated P_1 at 1–10 $\mu\text{C/m}^2$ (0.3–3 CGS units), and obtain the magnetoelectric contribution to the permittivity and magnetoelectric permeability of $PrFe_3(BO_3)_4$ in the form $4\pi\Delta\chi^e_{\text{rot}} = 1.1(10^{-6}–10^{-4})$ and $4\pi\sqrt{\chi_\perp\Delta\chi^e_{\text{rot}}} = 0.88(10^{-4}–10^{-3})$, respectively. As a result, the resonance angle of rotation of a polarization plane at an AFMR frequency of about 4 cm^{-1} is estimated at $\Delta\theta_{me} = 0.5°–5°$ for a thickness of 0.5 mm. Unfortunately, our quasi-optical investigations of c-cut $PrFe_3(BO_3)_4$ in crossed polarizers did not reveal polarization plane rotation, which is likely to be caused by a relatively low magnitude of the effect and an insufficiently high spectrometer sensitivity.

The easy-plane state also exhibits a resonance contribution to the electric and magnetoelectric susceptibilities, which is also determined by the susceptibility of rotation $\Delta\chi^e_{\text{rot}}$ in the region of a high-frequency (quasi-antiferromagnetic) AFMR mode and leads to electrical activity of this mode (i.e., excitation by an electric field), elliptical polarization of the corresponding electromagnetic eigenmodes in a crystal, and the rotation of the polarization plane of a propagating wave. However, in contrast to the previous case, all these effects are quadratic in small magnetoelectric constant c_1, which is likely to complicate the possibility of their observation. The manifestation of a magnetoelectric contribution in the region of a low-fre-

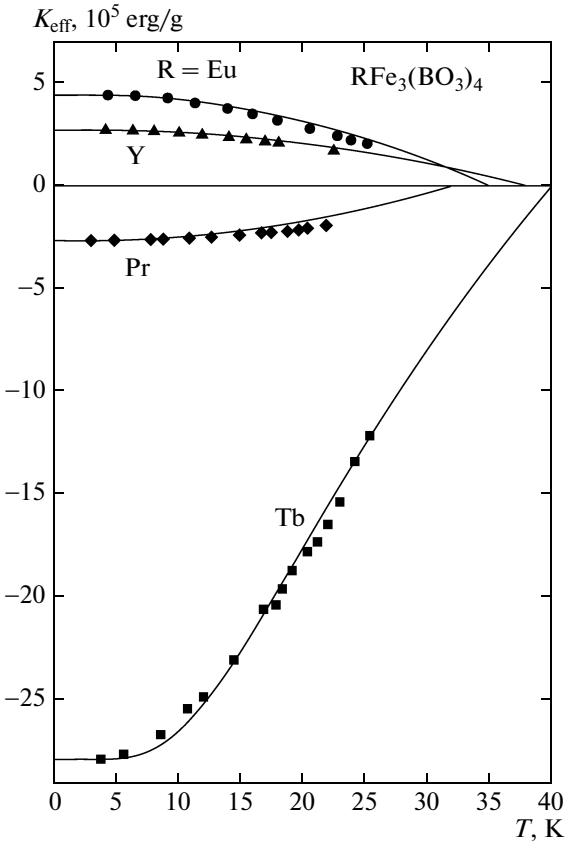

Fig. 6. Temperature dependences of the effective anisotropy constants of easy-plane (R = Y, Eu) and easy-axis (Pr, Tb) ferroborates: (points) values obtained upon the conversion of the experimental AFMR frequencies and mode contributions and (curves) theory.

quency mode seems to be more realistic; however, it requires a separate investigation. Note also that, since the rare-earth subsystem in a number of ferroborates can significantly contribute to the magnetoelectric interaction (polarization), one can expect a stronger manifestation of the dynamic effects considered above in the region of the corresponding rare-earth modes induced by transitions between the energy levels of an R ion.

CONCLUSIONS

When performing quasi-optical studies of rare-earth ferroborate $RFe_3(BO_3)_4$ (R = Y, Eu, Pr, Tb, $Tb_{0.25}Er_{0.75}$) single crystals in the submillimeter range ($\nu = 3–20$ cm^{-1}), we determined anisotropic permittivity ε', revealed its anomalies during structural phase transitions, and detected and investigated AFMR in the iron ion subsystem. We found a strong dependence of the AFMR frequency on the magnetic anisotropy and the character of the ground state of a rare-earth ion in crystal and exchange fields. Based on the data obtained for AFMR frequencies and the contributions of modes to the magnetic permeability, we determined the basic parameters of the magnetic interactions in the ferroborates under study (Fe–Fe exchange field H_E, effective anisotropy constant K_{eff}, effective R–Fe exchange fields H_{R-Fe}, the exchange splitting of the ground state of a rare-earth ion). It was shown that the values of exchange field H_E are close for all compositions under study and that the effective anisotropy constants (whose temperature dependences are shown in Fig. 6) differ significantly for compositions with different R ions. The determined exchange and anisotropy parameters and the splitting of the ground state of a rare-earth element agree well with the data of static and optical measurements. It was shown that taking into account a magnetoelectric interaction results in a number of new interesting effects, whose detection requires additional experimental efforts.

ACKNOWLEDGMENTS

This work was supported by the Russian Foundation for Basic Research, project no. 10-02-00846.

REFERENCES

1. A. K. Zvezdin, S. S. Krotov, A. M. Kadomtseva, G. P. Vorob'ev, Yu. F. Popov, A. P. Pyatakov, L. N. Bezmaternykh, and E. A. Popova, Pis'ma Zh. Eksp. Teor. Fiz. **81** (6), 335 (2005) [JETP Lett. **81** (6), 272 (2005)].
2. A. K. Zvezdin, G. P. Vorob'ev, A. M. Kadomtseva, Yu. F. Popov, A. P. Pyatakov, L. N. Bezmaternykh, A. V. Kuvardin, and E. A. Popova, Pis'ma Zh. Eksp. Teor. Fiz. **83** (11), 600 (2006) [JETP Lett. **83** (11), 509 (2006)].
3. A. N. Vasiliev and E. A. Popova, Fiz. Nizk. Temp. (Kharkov) **32** (8), 968 (2006) [Low Temp. Phys. **32** (8), 735 (2006)].
4. A. M. Kadomtseva, Yu. F. Popov, G. P. Vorob'ev, A. P. Pyatakov, S. S. Krotov, K. I. Kamilov, V. Yu. Ivanov, A. A. Mukhin, A. K. Zvezdin, A. M. Kuz'menko, L. N. Bezmaternykh, I. A. Gudim, and V. L. Temerov, Fiz. Nizk. Temp. (Kharkov) **36** (6), 640 (2010) [Low Temp. Phys. **36** (6), 511 (2010)].
5. J. A. Campá, C. Cascales, E. Gutiérrez-Puebla, M. A. Monge, I. Rasines, and C. Ruíz-Valero, Chem. Mater. **9**, 237 (1997).
6. Y. Hinatsu, Y. Doi, K. Ito, M. Wakeshima, and A. Alemi, J. Solid State Chem. **172**, 438 (2003).
7. D. Fausti, A. A. Nugroho, P. H. M. van Loosdrecht, S. A. Klimin, M. N. Popova, and L. N. Bezmaternykh, Phys. Rev. B: Condens. Matter **74**, 024403 (2006).
8. M. N. Popova, J. Rare Earths **27**, 607 (2009).
9. E. A. Popova, N. Tristan, C. Hess, R. Klingeler, B. Büchner, L. N. Bezmaternykh, V. L. Temerov, and A. N. Vasil'ev, Zh. Eksp. Teor. Fiz. **132** (1), 121 (2007) [JETP **105** (1), 105 (2007)].
10. M. N. Popova, E. P. Chukalina, T. N. Stanislavchuk, and L. N. Bezmaternykh, J. Magn. Magn. Mater. **300**, e440 (2006).
11. M. N. Popova, T. N. Stanislavchuk, B. Z. Malkin, and L. N. Bezmaternykh, Phys. Rev. Lett. **102**, 187403 (2009); M. N. Popova, T. N. Stanislavchuk, B. Z. Malkin,

and L. N. Bezmaternykh, Phys. Rev. B: Condens. Matter **80**, 195101 (2009).

12. A. M. Kadomtseva, Yu. F. Popov, G. P. Vorob'ev, A. A. Mukhin, V. Yu. Ivanov, A. M. Kuz'menko, and L. N. Bezmaternykh, Pis'ma Zh. Eksp. Teor. Fiz. **87** (1), 45 (2008) [JETP Lett. **87** (1), 39 (2008)].
13. E. A. Popova, D. V. Volkov, A. N. Vasiliev, A. A. Demidov, N. P. Kolmakova, I. A. Gudim, L. N. Bezmaternykh, N. Tristan, Yu. Skourski, B. Büchner, C. Hess, and R. Klingeler, Phys. Rev. B: Condens. Matter **75**, 224413 (2007).
14. E. A. Popova, N. Tristan, A. N. Vasiliev, V. L. Temerov, L. N. Bezmaternykh, N. Leps, B. Büchner, and R. Klingeler, Eur. Phys. J. B **62**, 123 (2008).
15. A. K. Zvezdin, A. M. Kadomtseva, Yu. F. Popov, G. P. Vorob'ev, A. P. Pyatakov, V. Yu. Ivanov, A. M. Kuz'menko, A. A. Mukhin, L. N. Bezmaternykh, and I. A. Gudim, Zh. Eksp. Teor. Fiz. **136** (1), 80 (2009) [JETP **109** (1), 68 (2009)].
16. Yu. F. Popov, A. M. Kadomtseva, G. P. Vorob'ev, A. A. Mukhin, V. Yu. Ivanov, A. M. Kuz'menko, A. S. Prokhorov, L. N. Bezmaternykh, and V. L. Temerov, Pis'ma Zh. Eksp. Teor. Fiz. **89** (7), 405 (2009) [JETP Lett. **89** (7), 345 (2009)].
17. A. I. Pankrats, G. A. Petrakovskii, L. N. Bezmaternykh, and V. L. Temerov, Fiz. Tverd. Tela (St. Petersburg) **50** (1), 77 (2008) [Phys. Solid State **50** (1), 79 (2008)]; A. I. Pankrats, G. A. Petrakovskii, L. N. Bezmaternykh, and O. A. Bayukov, Zh. Eksp. Teor. Fiz. **126** (4), 887 (2004) [JETP **109** (4), 766 (2004)].
18. A. D. Balaev, L. N. Bezmaternykh, I. A. Gudim, V. L. Temerov, S. G. Ovchinnikov, and S. A. Kharlamova, J. Magn. Magn. Mater. **258–259**, 532 (2003).
19. *Submillimeter Dielectric Spectroscopy of Solids*, Ed. by G. V. Kozlov (Nauka, Moscow, 1990) [in Russian]; G. V. Kozlov and A. A. Volkov, Top. Appl. Phys. **74**, 51 (1998).
20. A. G. Gurevich, *Magnetic Resonance in Ferrites and Antiferromagnets* (Nauka, Moscow, 1973) [in Russian].
21. A. M. Balbashov, A. A. Volkov, S. P. Lebedev, A. A. Mukhin, and A. S. Prokhorov, Zh. Eksp. Teor. Fiz. **88** (3), 974 (1985) [Sov. Phys. JETP **61** (3), 573 (1985)].
22. G. H. Dieke, *Spectra and Energy Levels of Rare-Earth Ions in Crystals* (Wiley, New York, 1969).
23. K. Taylor and M. Darby, *Physics of Rare-Earth Solids* (Wiley, London, 1971; Mir, Moscow, 1974).
24. C. Ritter, A. Balaev, A. Vorotynov, G. Petrakovskii, D. Velikanov, V. Temerov, and I. Gudim, J. Phys.: Condens. Matter **19**, 196227 (2007).

Translated by K. Shakhlevich